Supporting Drivers in Keeping Safe Speed in Adverse Weather Conditions by Mitigating the Risk Level

Romain Gallen, Nicolas Hautière, *Member, IEEE*, Aurélien Cord, and Sébastien Glaser

***Abstract*—Overspeeding is both a cause and an aggravation factor of traffic accidents. Consequently, much effort is devoted to limiting overspeeding and, consequently, to increasing the safety of road networks. In this paper, a novel approach to computing a safe speed profile to be used in an adaptive intelligent speed adaptation (ISA) system is proposed. The method presents two main novelties. First, the 85th percentile of observed speeds (V_{85}), estimated along a road section, is used as a reference speed, which is practiced and practicable in ideal conditions. Second, this reference speed is modulated in adverse weather conditions to account for reduced friction and reduced visibility distance. The risk is thus mitigated by modulating the potential severity of crashes by means of a generic scenario of accidents. Within this scenario, the difference in speed that should be applied in adverse conditions is estimated so that the highway risk is the same as in ideal conditions. The system has been tested on actual data collected on a French secondary road and implemented on a test track and a fleet of vehicles. The performed tests and the experiments of acceptability show a great interest for the deployment of such a system.**

***Index Terms*—Cooperative systems, friction, risk, safe speed, visibility.**

I. Introduction

With 1.27 million deaths annually worldwide, road crashes are of major concern. They were the ninth source of deaths in the world and are expected to be the fifth source in 2030 in developed countries as in developing regions [1], [2]. Indeed, speed is cited as the first factor; it is considered to be the cause in one third of road crashes [3], [4], and it also impacts the severity of accidents. Many attempts at reducing road fatalities and injuries have been undertaken over the past 50 years, from speed limitations to seat belt use and drug enforcement. In the past decade, automated control of speeds has proven very efficient in reducing accidents in England, the Netherlands, and France. It is estimated to have helped reduce fatalities in France by 25% between 2003 and 2007 according to [5]. However, recent trends have shown stagnation, suggesting that it has reached its full potential for safety benefits.

The development of advanced driver assistance systems (ADASs) is a very active field of research in the automotive industry. Systems relying on proprioceptive sensors, such as the antilock braking system (ABS) or the electronic stability program, are widely integrated in today's cars. Other systems rely on exteroceptive sensors (e.g., light detection and ranging, radars, and cameras), such as lane departure warning, forward collision warning, traffic sign recognition, or advanced front lighting systems.

In this context, ADASs focusing on speed, such as intelligent speed adaptation (ISA) systems, are considered as having high potential for road safety [6], whatever their types (static versus dynamic) and modes (mandatory versus advisory), mainly because of the drop in the number of crashes due to average speed decrease, all other things being equal. This has been formalized first by Nilsson's power model between speed and accident probability [7], which is later reviewed in [8]. Other works, such as [9] and [10], confirm that crash incidence generally declines as a result of speed limit reduction. The second reason for considering ISA as beneficial is the impact of speed on crash severity. Lower speeds mechanically lead to less severe accidents.

ISA systems can work in advisory or mandatory modes. Mandatory modes have only been tested in research projects such as [11]–[13]. The safety benefits of ISA systems are estimated to be higher for a dynamic ISA system in that mode (-44% of fatality) compared with the advisory mode (-9% of fatality) in the case of full penetration of ISA according to [14]. However, recent estimations of safety benefits for ISAs in France [15] have shown lesser potential, ranging from 4% to 16%, depending both on the mode and the type of road. Current implementations of ISA systems compliant with road regulation already exist in advisory mode in many cars with the use of speed limit detection algorithms using cameras, such as in [16].

Road design and legal speed limits are strongly linked. New roads are designed according to an iterative process between the needs and building constraints. Curvature, slope, and superelevation of the road are consistent with the foreseen speed limit. Secondary roads are often ancient and have been created before recent design models were created, presenting very tight curves, i.e., sections with a low sight distance for instance. Two thirds of road fatalities in France happen on secondary roads, and one third of the fatalities involve a single vehicle. Only road signs and speed limit signs are then used to inform the driver about the difficulties of the infrastructure characteristics

Manuscript received May 28, 2012; revised February 4, 2013 and April 30, 2013; accepted May 5, 2013. Date of publication May 27, 2013; date of current version November 26, 2013. This work was supported by the French National Research Agency under the DIVAS Project. The Associate Editor for this paper was H. Dia.

R. Gallen is with Centre d'Etudes Techniques Maritimes et Fluviales, Plouzané 28280, France (e-mail: romain.gallen@developpement-durable.gouv.fr).

N. Hautière is with the Laboratory for Road Operation, Perception, Simulations and Simulators, French Institute of Science and Technology for Transport, Spatial Planning, Development and Networks (IFSTTAR), Champs-sur-Marne 77420, France (e-mail: nicolas.hautiere@ifsttar.fr).

A. Cord and S. Glaser are with the Laboratory on Interaction between Vehicle Infrastructure and Driver, IFSTTAR, Versailles 78000, France (e-mail: aurelien.cord@ifsttar.fr; sebastien.glaser@ifsttar.fr).

Color versions of one or more of the figures in this paper are available online at http://ieeexplore.ieee.org.

Digital Object Identifier 10.1109/TITS.2013.2262523

to help him adapt his practiced speed. Because they are static and localized, the posted speed limits are not adaptive enough to build accurate safety measures. Sometimes, at a local scale, the posted speed limit should be seen as a legal speed limit but should not be considered as an advisable speed, particularly in adverse meteorological conditions when visibility or friction is reduced.

Among recent developments are adaptive dynamic ISA systems, whose aim is to cope with various conditions, particularly road curvature, lower friction, and poor visibility. Finding a safe speed recommended for a single driver in various conditions remains a challenging issue [17]. Curve warning systems (CWSs) can adapt speed in curves if the speed limit is not suitable, such as in [18] and [19]. The principles for the implementation of an ISA in adverse conditions have been proposed in [20] and [21]. These last two methods are based on the same safety criterion. The driver must be able to stop the vehicle in the visibility distance on wet, slippery, or dry roads.

In the cooperative framework of an adaptive and dynamic ISA system, this paper presents the onboard computation of a safe speed in real time along an itinerary. On one side, contextual information on conditions, such as fog [22], [23], rain [24], [25], or a wet road [26], is estimated in real time by in-vehicle sensors. On the other side, roadway information is used (reference speed, curvature, slope, or superelevation) to expand the electronic horizon before the car. This information is then fused online, and the reference speed is modulated depending on the environmental and geometric characteristics of the roadway. Our method is original in that the safe speed is not computed from models (a bottom-up approach such as in [21]) but, instead, by modulating a reference speed that is practiced and practicable in good conditions (a top-down approach), to get the same risk in adverse weather conditions as in good weather conditions. The proposed safety criterion, which is called the equivalent total risk (ETR) strategy, takes into account the potential severity of a crash using accident statistics. It is new and less constraining compared with the "stopping distance" or "zero risk" strategy used in [20] and [21]. The presented method is generic enough to be open and adaptable to specific vehicles, drivers, or road networks if one provides the corresponding inputs to the system.

This paper is organized as follows. Section II defines the concept of highway risk and the materials needed to implement this definition, namely, one crash severity metric and one emergency braking model. In Section III, the proposed risk mitigation based on the ETR criterion is presented and is applied at one point on the road for a given severity level. In Section IV, the ETR strategy is applied with simulated adverse conditions along an actual road section on which the characteristics and reference speed have been collected. In Section V, the output of the system on a real path is shown and analyzed. Finally, Section VI presents the conclusion and the next steps of this paper.

II. Highway Risk

Here, the concept of highway risk is defined. Then, the materials needed to implement this definition are detailed: crash severity metrics and an emergency braking model. Ultimately, due to these different elements, the notion of risk level can be mathematically defined.

A. Definition of Highway Risk

Risk can be defined as the combination of the probability of an accident with its severity. Our risk definition is based on a basic scenario of accident. While the case vehicle is driving in free-flow conditions, an emergency situation occurs. The driver begins an emergency braking maneuver and eventually crashes against a rigid fixed obstacle. The emergency situation, whatever its cause (distraction or surprise), may happen anywhere during the trip. In this scenario, it is considered that there is an equiprobability of obstacle appearance depending on the distance. The driver may run off the road anytime after the detection of an emergency situation and then hit an obstacle. In this scenario, the driver brakes on the road and hits an obstacle on the carriageway or on the roadside. As the friction outside the road is assumed to be negligible, the driver hits the obstacle with the same speed that he had when he ran off the road. The severity of the accident depends on the speed of the crash, the nature of the obstacle, and the hitting configuration, as defined in the following.

B. Crash Severity Metrics

The potential severity of an accident depends on the speed of a crash and on its configuration (frontal collision with a rigid fixed object, with another vehicle, or with a stopped vehicle). Many studies have described the link between the speed of crashes and the severity for the driver or for other vehicle occupants. This severity may depend on driver characteristics such as age, gender, or weight [3], [27], on the vehicle safety devices [28], [29], on the direction of collision [30], on the mass ratio in two-vehicle crashes [31], or on the size of cars [32].

Many different metrics linked to speed are used to assess the potential severity of crashes. These are the kinetic energy equivalent speed (KEES or EES), the equivalent barrier speed, the occupant impact velocity (OIV), or the acceleration severity index (ASI). In [33], the severity of an accident is described using the maximum accident injury severity and the variation of speed during the accident for both frontal and side impacts. Some of these measures were designed to relate vehicle kinematics at the instant of a crash (derived from postcrash observation of vehicle deformation), whereas other speed-related parameters were designed to study potential injury severity. They can be computed with data from postcrash analysis of vehicles or, nowadays, from event data recorders integrated in cars. The OIV and the ASI were found by [34] to offer no significant predictive advantage over the simpler delta-V (ΔV). Delta-V is an indication of the acceleration experienced by car occupants, whereas EES assesses the work done in crushing the car structure [35].

According to [36], from the analysis of collision data for Britain, Australia, and the U.S., all collisions can be considered frontal impacts for high collision severity levels (i.e., high ΔV values). The risk for vehicle occupants is

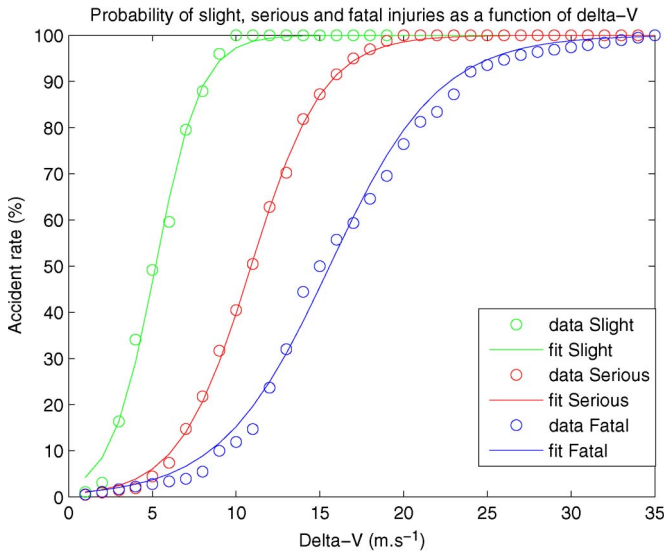

Fig. 1. Cumulative speed curves for drivers in frontal impacts, data from [37], and curve fitting.

TABLE I
COEFFICIENTS OF FITTING FOR PI CURVES DEPENDING ON SEVERITY, AS SHOWN IN FIG. 1

Severity	Coefficients		
Slight	$a_{Sl} = 100$	$b_{Sl} = 5.19$	$c_{Sl} = 1.34$
Serious	$a_{Se} = 100$	$b_{Se} = 10.9$	$c_{Se} = 2.15$
Fatal	$a_{Fa} = 100$	$b_{Fa} = 15.6$	$c_{Fa} = 3.26$

estimated by using statistics giving injury severity probability as a function of delta-V in frontal impacts taken from [37], as shown in Fig. 1.

To dispose of continuous cumulative crash severity curves depending on delta-V, sigmoid functions were fitted to the data from [37]. They are of the logit form, i.e.,

$$\mathrm{PI}_{\mathrm{Severity}}(\Delta V) = \frac{a_{\mathrm{Severity}}}{1 + e^{\frac{-\Delta V - b_{\mathrm{Severity}}}{c_{\mathrm{Severity}}}}} \tag{1}$$

where a, b, and c are coefficients that vary based on the severity, which can be either slight, serious, or fatal. There are three sets of coefficients given in Table I, one for each probability of injury (PI) curve, such as shown in Fig. 1.

C. Emergency Braking Model

Any model of infrastructure–driver–car interactions able to compute a braking speed profile in emergency situations could be used in the framework that we propose. The proposed model is simple and illustrative of our capabilities to account for infrastructure, vehicle, and driver characteristics that we measured and were able to feed the system as inputs. The speed profile during an emergency braking is computed using measured local characteristics of the road, such as curvature, slope angle, superelevation, and friction, as presented in Section IV-B. Driver-related parameters, such as reaction time and pressure on the brake pedal, are also used in the model of the vehicle dynamics. Finally, vehicle-related parameters, such as the presence of an ABS, are used to compute these speed profiles.

After an emergency situation arises, the driver needs some time to be aware of the situation and to start pressing the brake pedal. During this time of perception and reaction, the speed is kept constant, and the distance D_{Reac} covered is

$$D_{\mathrm{Reac}} = V_0 t_{\mathrm{PR}} \tag{2}$$

where V_0 is the speed (in $\mathrm{m \cdot s^{-1}}$) and t_{PR} is the perception–reaction time (in seconds). Once the driver has covered this distance with constant speed, the emergency braking takes place with a starting speed equal to V_0. The emergency braking speed profiles are computed differently on straight sections and in curves.

1) Braking on Straight Sections: On straight sections, the mobilized friction can be entirely used for the longitudinal braking procedure. The acceleration is expressed as a fraction of g, which is the acceleration of gravity ($g = 9.81\ \mathrm{m \cdot s^{-1}}$). The maximum longitudinal acceleration is

$$\mathrm{Acc}_{\mathrm{Lon}}(x) = \mathrm{Acc}_{\mathrm{Tot}}(x) = -g\left(\mu(x) + s(x)\right) \tag{3}$$

where x is the curvilinear abscissa on the road, $\mu(x) \in [0,1]$ is the friction according to abscissa, and $s(x)$ is the slope rate according to position (positive for an upslope).

The actual acceleration resulting from braking is computed from the mobilized longitudinal acceleration with

$$\mathrm{Acc}_{\mathrm{Mob}}(x) = \gamma \mathrm{Acc}_{\mathrm{Lon}}(x) = -\gamma g\left(\mu(x) + s(x)\right) \tag{4}$$

where $\gamma \in [0, 1]$ is a parameter linked to the driver's pressure on the brake pedal and the presence of an ABS in the vehicle. $\gamma = 0.9$ is used when the car has an ABS, and $\gamma = 0.7$, otherwise [38], [39].

2) Braking in Curves: While braking on straight sections allows the driver to mobilize all friction and energy in stopping, braking in curves requires mobilizing part of the friction to follow the path. The stopping distance is thus longer than on straight parts of the road. A model of the vehicle dynamics is used to account for trajectory keeping. Lateral acceleration depends on the curvature of the road and on the speed. The maximal lateral acceleration is defined as

$$\mathrm{Acc}_{\mathrm{Lat}}(x) = \left|\frac{V(x)^2}{R(x)}\left(\mu(x) + \varphi(x)\right)\right| \tag{5}$$

where $R(x)$ is the radius of the curve depending on the curvilinear abscissa (positive in left turns, negative in right turns), and $\varphi(x)$ is the superelevation angle (positive if the center of the lane is higher than the outside). This corresponds to the part of friction mobilized to keep the trajectory. Given a certain amount of friction available, the total deceleration is bounded as follows:

$$\mathrm{Acc}_{\mathrm{Tot}}(x) = \sqrt{\mathrm{Acc}^2_{\mathrm{Lon}}(x) + \mathrm{Acc}^2_{\mathrm{Lat}}(x)}. \tag{6}$$

The mobilized longitudinal acceleration that remains after braking is

$$\mathrm{Acc}_{\mathrm{Lon}}(x) = -\sqrt{\left(g\left(\mu(x) - s(x)\right)\right)^2 - \left(\frac{V(x)^2(\mu(x)+\varphi(x))}{R(x)}\right)^2}. \tag{7}$$

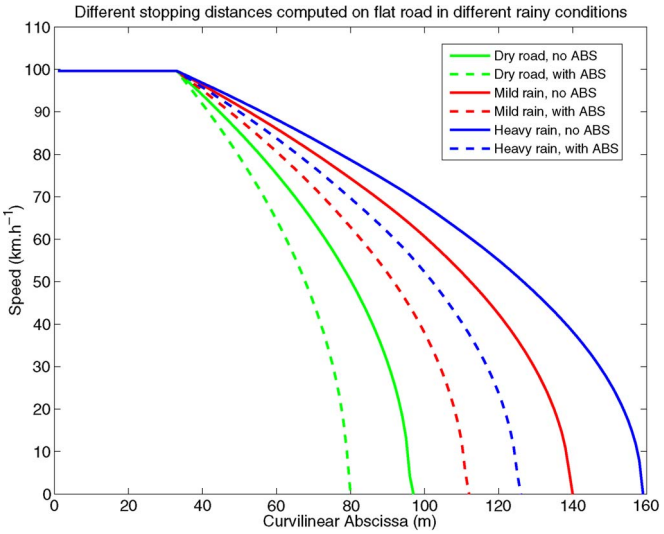

Fig. 2. Emergency braking speed profiles under various rainy conditions.

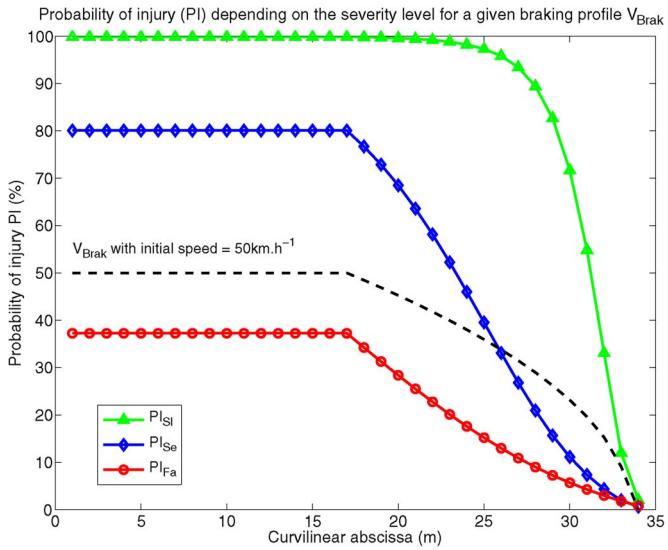

Fig. 3. Braking speed profile V_{Brak} with parameters ($V_0 = 50$ km $\cdot$ h^{-1}, $t_{\mathrm{PR}} = 1.2$ s, $\mu(x) = \mu_{dry}(x) \in [0.8, 0.9]$, and $\gamma = 0.9$) and corresponding curves of the PI, i.e., $\mathrm{PI_{Sl}}$, $\mathrm{PI_{Se}}$, $\mathrm{PI_{Fa}}$.

Similar on straight lines, the real deceleration produced by braking is computed by correcting the mobilized longitudinal acceleration with the brake pedal pressure and ABS-related parameter γ, i.e.,

$$\mathrm{Acc_{Mob}}(x) = -\gamma\sqrt{\left(g\left(\mu(x) - s(x)\right)^2 - \left(\frac{V(x)^2\left(\mu(x) + \varphi(x)\right)}{R(x)}\right)^2}. \tag{8}$$

Notice that (8) reduces to (4) on straight sections where $R(x) = \infty$.

3) Braking Speed Profile: The mobilized longitudinal acceleration during braking at each position along straight sections and curves is known with (4) and (8), respectively. The accurate speed profile during braking $V_{\mathrm{Brak}}(x)$ is computed, given step $dx = 1$ m with an iterative procedure. For each position until $V(x) = 0$ (i.e., the vehicle has completely stopped) the following equation is solved:

$$\frac{V_{x+dx}^2 - V_x^2}{2dx} = \mathrm{Acc_{Mob}}(x). \tag{9}$$

Knowing the static characteristics of the road ahead, i.e., $R(x)$, $s(x)$, and $\varphi(x)$, given fixed parameters linked to the vehicle and the driver, i.e., t_{PR} and $\gamma(x)$, and for a given position x on the road, a braking speed profile can be computed using (9). The complete profile of speed during an emergency braking is then composed between the initial position and the total stopping distance D_S, as shown in Fig. 2. The total stopping distance D_S covered from the start of the emergency situation to the complete stop of the vehicle is such that

$$D_S = D_{\mathrm{Reac}} + D_{\mathrm{Brak}}. \tag{10}$$

As an example, we can foresee the influence of a wet road on road safety. Wet road is a major issue for traffic safety as it means reduced pavement friction. French statistics of crashes [5] show an increase in the number of accidents under rainy conditions. Although drivers are often confronted with those conditions, they are not aware of the impact of different rainy conditions on braking distance and trajectory keeping. The speed profile is the concatenation of a constant speed part of length D_{Reac} and the braking profile $V_{\mathrm{Brak}}(x)$ of length D_{Brak}, as shown in Fig. 2. It illustrates different speed profiles computed for the same driver ($t_{\mathrm{PR}} = 1.2$ s) on a car with and without an ABS in increasing rainy conditions. The total stopping distance is almost doubled depending on the presence of an ABS and the intensity of rain.

D. Deducing Risk Level

Fig. 3 shows the probability of slight, serious, and fatal injury ($\mathrm{PI_{Sl}}$, $\mathrm{PI_{Se}}$, and $\mathrm{PI_{Fa}}$) computed for the emergency braking superimposed on the figure as a dashed black line with the curves of the PI shown in Fig. 1. The different estimations of PI are computed according to (1) with the coefficients given in Table I. The PI for a crash ahead of the vehicle is

$$\mathrm{PI_{Severity}}(x) = \mathrm{PI_{Severity}}\left(V_{\mathrm{Brak}}(x)\right). \tag{11}$$

Fig. 3 shows how the resulting PI is computed for a given profile of V_{Brak}. These PI curves can be computed for the three levels of severity at each instant on the road. If such an emergency situation occurs right in front of the vehicle, this means that the probability of an incident or an accident is equal to 1. By considering the definition of highway risk given in Section II-A, we can state that the risk level at a given abscissa equals the PI.

III. Risk Mitigation Method

Earlier, the highway risk has been mathematically defined. The principle of our method is then to keep the risk for the driver in adverse conditions equal to the reference risk (i.e., the risk in good weather conditions). In this aim, two speed profiles during emergency braking are computed. One profile is

computed with good friction and good visibility conditions, and the other profile is computed with adverse conditions detected in real time (such as rain that may reduce friction and/or visibility such as fog that impacts mainly on visibility).

A. Existing Approaches

Existing approaches such as [20] and [21] focus on stopping before hitting an obstacle on the road. This strategy of handling risk has three major issues. First, in an emergency situation, the driver may run off the road near an obstacle and hit it with high speed. Distant obstacles are not the most dangerous obstacles. The second issue is that trying to avoid any contact with the obstacle can be considered "zero risk" strategy, whereas a low-speed crash may not be of severe consequences. The third issue is that a too cautious strategy may end up advising a speed much lower than the legal speed, thus lowering the credibility of the advice and lessening the efficiency of the ISA system.

The use of a "zero risk" strategy is shown in Fig. 5 on a wet road and in Fig. 7 in a foggy condition. On wet roads, this approach would lead to lowering the initial speed so that the stopping distance $d_{\mathrm{S-Cur}}$ is the same as on dry road $d_{\mathrm{S-Ref}}$. In a foggy condition, this approach would lead to lowering the initial speed so that the stopping distance $d_{\mathrm{S-Cur}}$ equals the visibility distance d_{Vis}.

B. Novel Approach

Our novel approach consists in lowering initial speed in adverse conditions (reduced friction or reduced visibility) in such a way that the total PI in adverse conditions equals the total PI in reference conditions, all else being equal, i.e.,

$$\int_0^{d_{\mathrm{S-Ref}}} \mathrm{PI}(V_{\mathrm{Brak-Ref}})dx = \int_0^{d_{\mathrm{S-Cur}}} \mathrm{PI}(V_{\mathrm{Brak-Adv}})dx. \quad (12)$$

In the following, we show the result of this ETR approach at one point of the road in rainy and foggy conditions for a given severity level.

C. Risk Mitigation in Rain: One Severity Level

The ETR strategy is shown in rainy weather in Figs. 4 and 5 at one point of the road. A dichotomic procedure is applied to find an initial speed in adverse conditions such that the total probability of fatal injuries during braking is equivalent to the total reference probability of fatal injuries, as proposed in (12), all else being equal.

Fig. 4 shows the fatal PI curve in reference conditions for a driver at reference speed $V_{\mathrm{Ref}} = 90$ km $\cdot$ h^{-1} on a dry road with $\mu_{\mathrm{Ref}} \in [0.83, 0.88]$ on this section of the road (plain blue line). At first, the fatal PI (dotted red line) for the current conditions is estimated with $V_{\mathrm{Cur}} = 90$ km $\cdot$ h^{-1} on a wet road with a water height of 1 mm ($\mu_{\mathrm{Cur}} \in [0.47, 0.51]$). If the total current $\mathrm{PI}_{\mathrm{Fa-Cur}}$ is superior to the reference $\mathrm{PI}_{\mathrm{Fa-Ref}}$, an advisory speed $V_{\mathrm{Adv}} = 81$ km $\cdot$ h^{-1} is computed such that total $\mathrm{PI}_{\mathrm{Fa-Adv}}$ with advisory speed (dot–dashed green line) equals

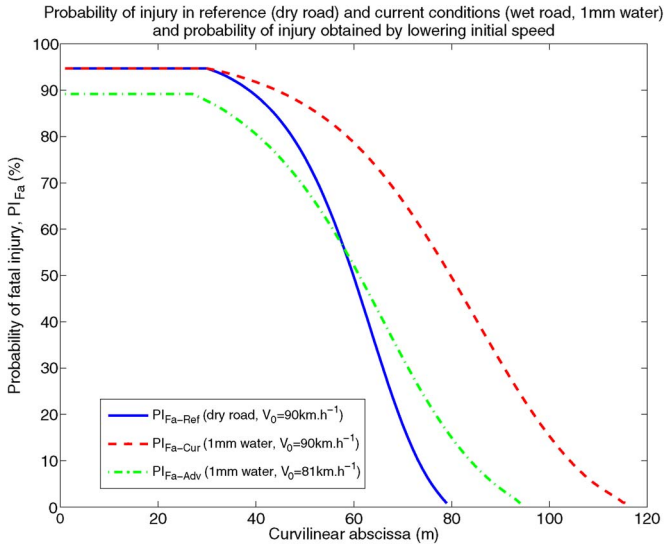

Fig. 4. Probability of fatal injuries $\mathrm{PI}_{\mathrm{Fa}}$ for emergency braking on a wet pavement at 90 km $\cdot$ h^{-1}.

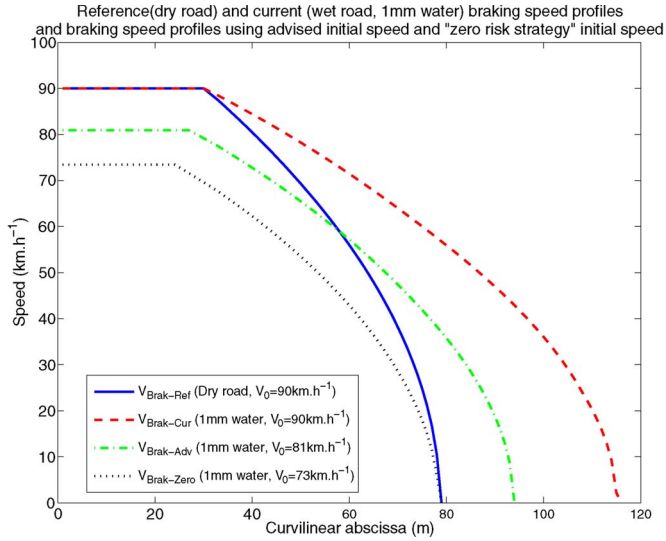

Fig. 5. Emergency braking speed profiles in rain at one point on the road.

total reference $\mathrm{PI}_{\mathrm{Fa-Ref}}$. Notice that, with our advisory speed, the stopping distance is slightly longer than in the reference conditions (93 versus 79 m).

Fig. 5 shows the different emergency braking speed profiles that would occur in the different conditions and using the different advisory strategies. The braking speed profile using the "zero risk" strategy, such as proposed in [20] and [21] (dotted black line), is also presented for comparison. Using this method leads to an advisory speed such that the stopping distance equals the reference stopping distance (79 m). As expected, such a strategy would lead to the lowest advisory speed ($V_{\mathrm{Zero}} = 73$ km $\cdot$ h^{-1}).

At any given point along the road, the risk in the current situation and the risk in the reference situation are compared. From this comparison, a lower speed can be proposed, which brings the current risk down to the same level as the reference risk. It is interesting to note that the advised speed is actually that recommended in the driving manuals for rainy weather

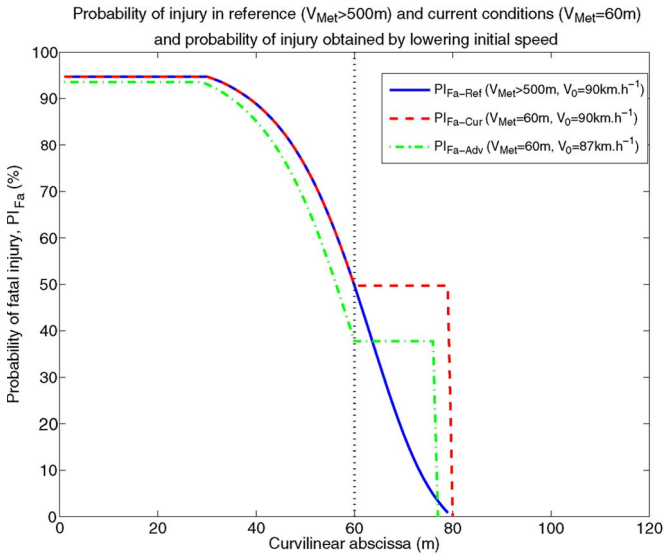

Fig. 6. Braking speed profile and probability of fatal injuries in fog with 60 m of visibility distance.

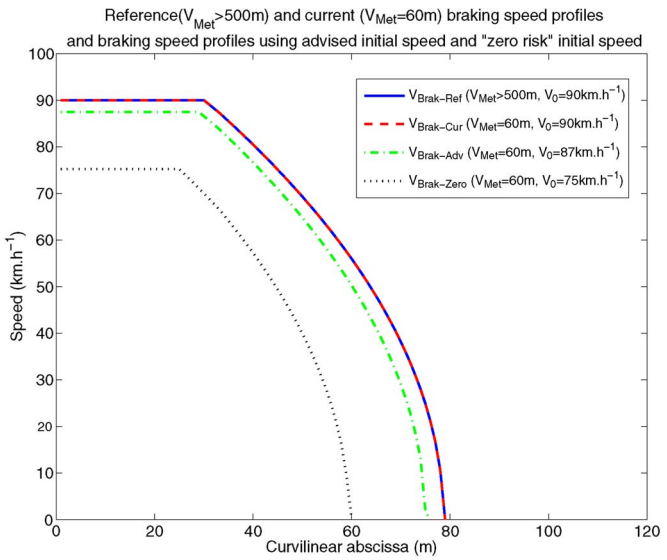

Fig. 7. Emergency braking speed profiles in fog at one point on the road.

on rural highways ($90\ \mathrm{km \cdot h^{-1}} \rightarrow 80\ \mathrm{km \cdot h^{-1}}$). Our strategy can be applied for each level of severity, giving three different advised speeds with which the total risk in adverse conditions of friction equals the total risk in reference conditions for that level of severity.

D. Risk Mitigation in Fog: One Severity Level

Fog essentially impairs highway visibility. French statistics of crashes [5] show that it increases the average severity of crashes, meaning drivers collide with obstacles at higher speeds. Potential severity calculations are adapted by considering that the PI is constant beyond the visibility distance as shown in Fig. 6. The PI depending on severity is set constant from the visibility distance up to the total stopping distance. This has no impact if the braking speed profile produces a total stopping distance lower than the visibility distance. Our ETR strategy is applied at this point of the road, and a dichotomic procedure is then applied to find an initial speed in adverse conditions such that the total probability of fatal injuries during braking is equivalent to the total reference probability of fatal injuries, all else being equal.

Fig. 6 shows the fatal PI curve in the reference conditions (plain blue line) for a driver at reference speed $V_{\mathrm{Ref}} = 90\ \mathrm{km \cdot h^{-1}}$ on a dry road with $\mu_{\mathrm{Ref}} \in [0.83, 0.88]$. In this example, considering that the fog only impacts on visibility, the current braking speed profile is identical to the one in the reference conditions $V_{\mathrm{Brak-Cur}} = V_{\mathrm{Brak-Ref}}$. Nevertheless, the current fatal PI computed for that braking profile is modified such that $\mathrm{PI_{Fa}}(x > V_{\mathrm{Met}}) = \mathrm{PI_{Fa}}(V_{\mathrm{Met}})$ (dashed red line). With the total current $\mathrm{PI_{Fa-Cur}}$ being superior to the reference $\mathrm{PI_{Fa-Ref}}$, an advisory speed $V_{\mathrm{Adv}} = 87\ \mathrm{km \cdot h^{-1}}$ is computed such that the total $\mathrm{PI_{Fa-Adv}}$ with advisory speed (dot–dashed green line) equals the total reference $\mathrm{PI_{Fa-Ref}}$.

Fig. 7 shows the different emergency braking speed profiles that would occur with the reference and advised speeds computed using the different strategies. The profile resulting from using the "zero risk" strategy (dottted black line) is also presented for comparison. Using this method leads to an advisory speed such that the stopping distance equals the meteorological visibility distance ($V_{\mathrm{Met}} = 60$ m). As expected, this strategy would lead to the lowest advisory speed ($V_{\mathrm{Zero}} = 75\ \mathrm{km \cdot h^{-1}}$).

At any given point along the road, the risk in the current situation and the risk in the reference situation are compared. From this comparison, a lower speed can be proposed to bring the current risk down to the same level as the reference risk. Our strategy can be applied for each level of severity, giving three different advised speeds with which the total risk in adverse conditions of visibility equals the total risk in the reference conditions for that level of severity, all else being equal.

Using the method exposed earlier for rainy or foggy situations leads to different advised speeds depending if one focuses on ETR for slight, severe, or fatal injuries. We illustrated our strategy with the fatal injury criterion, but the method is identical with other criteria.

We next show how we compose different speed recommendations depending on the severity of the injury criterion considered.

IV. Risk Mitigation Along a Road Section

Earlier, a risk mitigation strategy, which is called ETR, was presented and applied at one point of a road in the case of reduced friction or visibility. Here, the ETR strategy is applied on an actual road section with simulated weather conditions. A road itinerary of 40 km was selected in the network of the Conseil Général (CG 22) of Côtes d'Armor (RD 786) in western France. On this section, infrastructure parameters were collected, and a V_{85} speed profile was measured in ideal conditions to be used as the reference speed profile.

A. Estimation of a Reference Speed

The V_{85} speed is the 85th percentile of a speed distribution; it is usually measured in ideal meteorological conditions. This

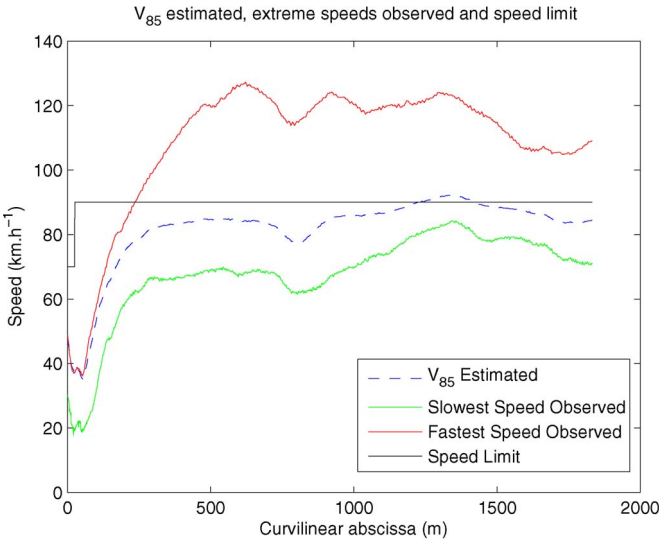

Fig. 8. Estimated V_{85} speed profile, extreme speeds observed, and speed limit on a portion of the RD786 of CG 22 (France).

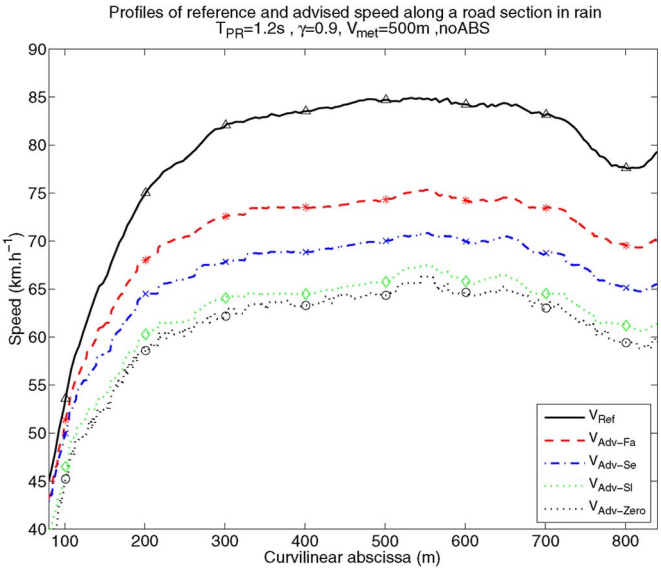

Fig. 9. Profiles of advised speeds computed with different safety criteria on a wet road.

definition is widely used in roadway engineering, either for design or safety purposes, although it depends on the way it is measured. It depends on the nature of vehicles taken into account (light vehicles, trucks, etc.) and also if the vehicle is in traffic or in free flow (3–10 s from the preceding vehicle). Its estimation could be erroneous if the moment and the integration time of the measurements are not carefully chosen. This speed is practiced and practicable in the same conditions as the measuring conditions (by light vehicles in free flow in our example).

Unlike usual measures of V_{85} collected at one spot, a continuous profile of V_{85} along a path is used. This profile of reference speed can be computed with the methodology presented in [40]. To get this profile, several real-driving sessions are needed during daytime and nighttime. Profiles where the measuring car is constrained by traffic need to be discarded (night sessions are easier in this respect). The test drivers are asked to follow the path with either normal or hurried speed. Fig. 8 shows two extreme profiles observed (the slowest profile and the fastest profile), the posted speed limit, and the estimated V_{85} profile.

On secondary roads, for a vehicle in free-flow conditions with ideal meteorological conditions, the V_{85} profile is a more realistic and acceptable speed to be advised than the regulatory speed. For legal purposes, it may be necessary for the reference speed to comply with the posted speed limits. The reference speed to be used can be defined as the estimated V_{85} as long as it is lower than the posted speed limit.

B. Collection of Infrastructure Parameters

Geometric characteristics of the roads are of major importance concerning the dynamic behavior of the vehicles. Many "run-off-the-road" crashes are the consequences of a misunderstanding of the complex interaction between those characteristics and vehicle speed [4]. For example, most drivers do not know the impact of slope on the length of braking or the limits of controllability of their vehicle depending on their speed with respect to the road curvature in curves. A mapping vehicle can be driven along a road to gather information such as curvature, slope angle, and superelevation. These characteristics do not evolve in time. Once acquired, this information is available for the whole road. It could be embedded into cars through the use of maps. It could also be transmitted by the infrastructure using relevant vehicle-to-infrastructure (V2I) protocols. An electronic horizon of 300 m is sufficient to compute the emergency braking profiles according to the methodology detailed in Section III.

All the characteristics are not alike. Friction, which is a major characteristic of the road, is mainly linked to road roughness, tire nature (slick or engraved), and water height. Our measuring vehicle is able to estimate friction for a standard tire under 1 mm of water. This characteristic is assumed to be semi-static. The profile of friction can be transmitted to the car along with other characteristics of the road. Water height will be measured by roadside units (RSUs) due to dedicated devices and spatially refined in real time with cameras using algorithms, such as in [25], [26], and [41]. Then, using a model of friction estimation depending on water height, real friction can be estimated at any time near the car [42].

C. First Results of Risk Mitigation Along a Road Section

Fig. 9 shows the result of the methodology that leads to an advisory speed with our ETR strategy. Using this methodology allows us to propose, at a given position on the road, three different advisory speeds depending on the potential severity taken into account. Accounting for "slight injuries" leads to a more cautious speed than accounting for "fatal injuries." The advisory speeds computed with our method will be compared with the reference speed on a dry road (i.e., the V_{85} speed in good weather or V_{Ref}) and with the advisory speed computed with an existing method based on the "zero risk" strategy.

It is possible to compute different braking profiles under rainy conditions; it is also possible to compose these braking

profiles with the curves of the PI to propose an advisory speed along the road, as shown in Fig. 9.

Notice that the advisory speed taking into account slight severity injuries is very close to the advisory speed proposed with the "zero risk" strategy proposed in [20] and [21]. This was expected because slight injury curves are very sharp for low speeds and saturated over 10 $\mathrm{m}\cdot\mathrm{s}^{-1}$ (see Fig. 1). This means that only the end of the braking speed profile is used to compensate for the ETR strategy. The "zero risk" strategy can be assimilated to an ETR strategy with a severity curve equal to 100% from $\Delta V = 1\ \mathrm{m}\cdot\mathrm{s}^{-1}$ (100% probability of severity whatever the speed of the crash, meaning the crash should be absolutely avoided).

D. Risk Mitigation for Different Severity Levels

In Fig. 3, the braking speed profile goes from a medium speed ($50\ \mathrm{km}\cdot\mathrm{h}^{-1}$) down to stop, and the different probabilities of injury between 37% and 100% at the beginning of the emergency braking go down to 0% at the end. This is the direct consequence of the application of the curves shown in Fig. 1. This means that, applying this composition on an emergency braking at high speed would lead to a $\mathrm{PI}_{\mathrm{Sl}}$ near 100% along most of the braking distance. Conversely, using such composition on a low-speed emergency braking ranging from 30 $\mathrm{km}\cdot\mathrm{h}^{-1}$ to stop would lead to a $\mathrm{PI}_{\mathrm{Fa}}$ near 0% along most of the braking distance.

This reflects the fact that, at high speeds, whatever the distance from the obstacle, the driver is highly susceptible to having at least a slight injury and that, at low speeds, it is highly improbable that he might suffer fatal injuries. Seeing this evidence, we consider that it is not of major importance to modulate the initial speed for fatal injuries when there is almost no risk of fatal injuries and for slight injuries when they are almost unavoidable. We automatically compose the advised initial speeds corresponding to different severity levels of injury criteria by accounting for the most relevant criterion that is emphasized. The weighting of the advised speed is computed according to (13), shown at the bottom of the page, where Severity stands for one of the severity criteria considered (slight, serious, or fatal), and $\overline{\mathrm{PI}_{\mathrm{Severity}}}$ is the mean value of the PI over the emergency braking distance.

Using (13), we compute at each point of the road three weighting factors, α_{Sl}, α_{Se}, and α_{Fa}, whose sum equals 1, and we advise a current speed recommendation according to

$$V_{\mathrm{Adv-final}} = \alpha_{\mathrm{Sl}}\cdot V_{\mathrm{Adv-Sl}} + \alpha_{\mathrm{Se}}\cdot V_{\mathrm{Adv-Se}} + \alpha_{\mathrm{Fa}}\cdot V_{\mathrm{Adv-Fa}}. \tag{14}$$

Fig. 10 shows the value of the weighting factors α used to weight the different advised speeds corresponding to different severity criteria depending on the current speed.

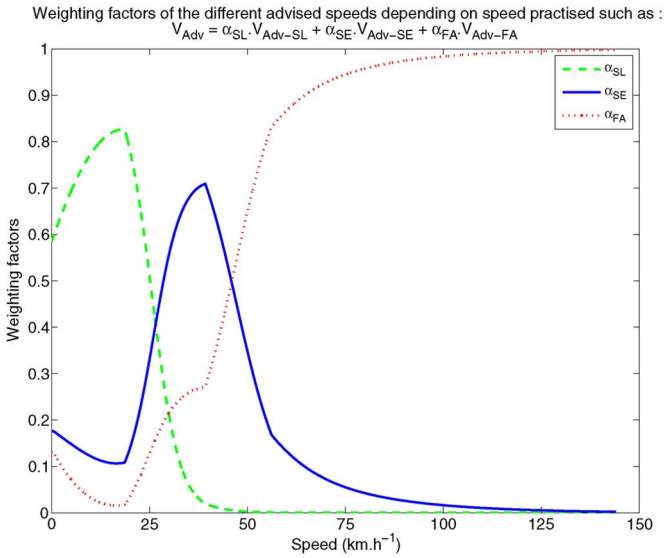

Fig. 10. Weighting of advised speeds linked to different severity levels.

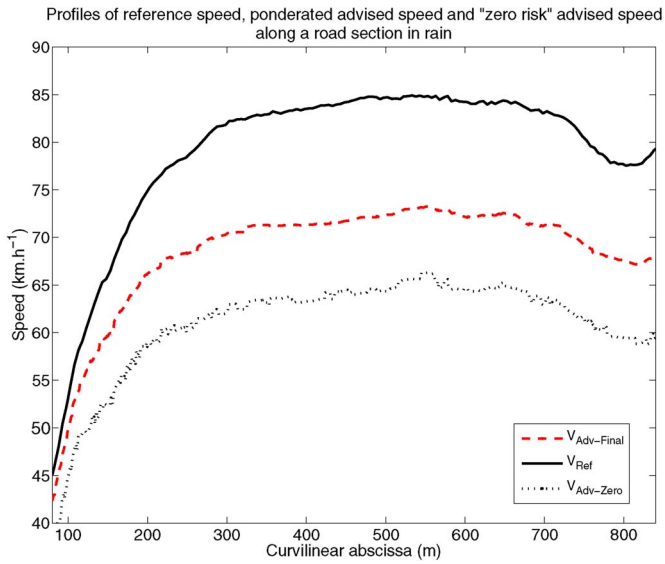

Fig. 11. Speed profiles under rainy conditions.

We showed how the advised speed can be computed at each point of the road depending on different adverse conditions and accounting for different levels of severity of injury. We showed how we compose the different advised speeds computed to propose a unique advised speed to the driver. In the following, the whole profiles of the advised speed along the road are presented depending on different adverse conditions.

E. Experimental Results

1) Reduced Friction on a Wet Road: We show in Fig. 11 the profile of our advised speed composed from the three advised

$$\alpha_{\mathrm{Severity}} = \frac{\min(\overline{\mathrm{PI}_{\mathrm{Severity}}},\ 100 - \overline{\mathrm{PI}_{\mathrm{Severity}}})}{\left(\min(\overline{\mathrm{PI}_{\mathrm{Sl}}},\ 100 - \overline{\mathrm{PI}_{\mathrm{Sl}}}) + \min(\overline{\mathrm{PI}_{\mathrm{Se}}},\ 100 - \overline{\mathrm{PI}_{\mathrm{Se}}}) + \min(\overline{\mathrm{PI}_{\mathrm{Fa}}},\ 100 - \overline{\mathrm{PI}_{\mathrm{Fa}}})\right)} \tag{13}$$

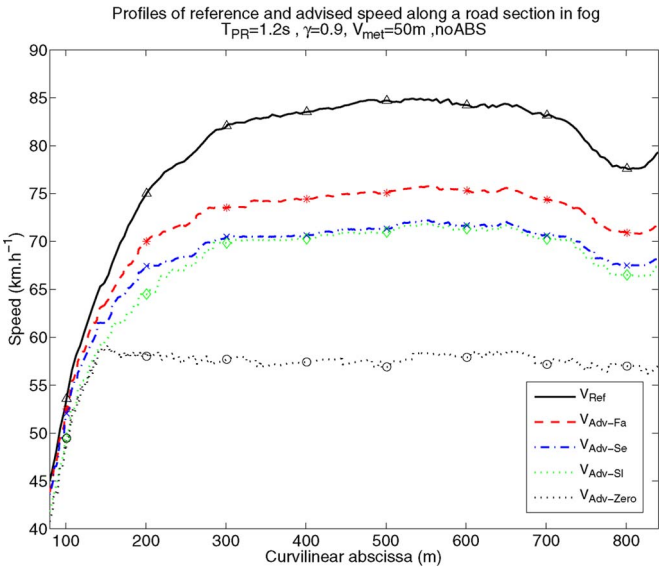

Fig. 12. Different speed profiles in fog with $V_{\mathrm{Met}} = 50$ m.

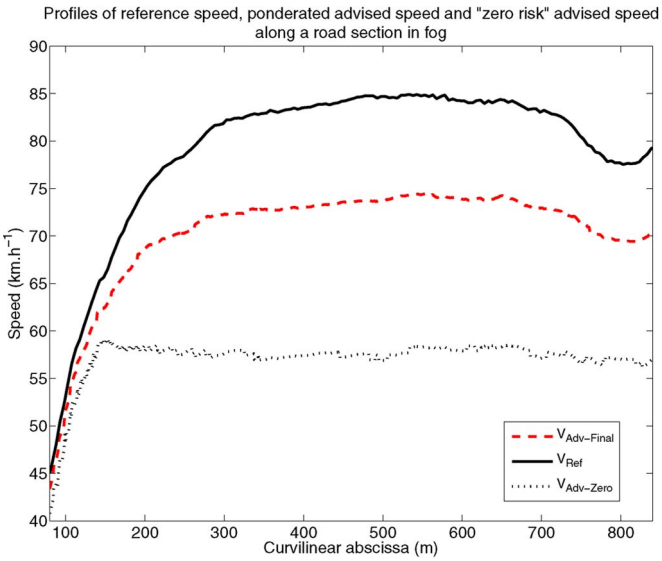

Fig. 13. Reference, "zero risk," and ETR speed profiles in fog with $V_{\mathrm{Met}} = 50$ m.

speeds shown in Fig. 9. At low speed, the profile tends to be closer to the speed advised to prevent slight injury, whereas at high speed, it is closer to the speed advised to prevent fatal injury.

2) Reduced Visibility in Fog: As shown in Fig. 11 for rainy situations, we computed three different advised speeds in fog using different safety criteria. The advisory speeds along the whole road are computed in the presence of fog limiting the visual range to 50 m, as shown in Fig. 12.

We computed a weighted advised speed according to the methodology presented in Section IV-D and as we did in Fig. 11 for a rainy situation. The final advised speed in a foggy situation is shown in Fig. 13.

Notice that, since the visual range is limited to a fixed distance, the speed proposed using the "zero risk" strategy is almost constant. The small variations are only due to road properties used in our model of the dynamics of the car ($p(x)$, $\mu(x)$, and $\phi(x)$). These small variations allow for the driver to always be able to stop within 50 m. Before an abscissa of 150 m, none of the strategies ("total risk" or "zero risk") have any impact on the initial speed since the initial speed is sufficiently low to allow for the driver to stop in less than 50 m.

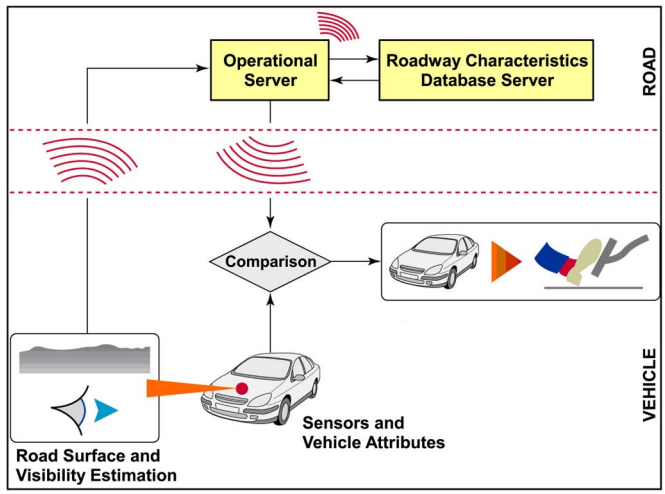

Fig. 14. Layout of VII in the DIVAS project.

We showed how we handle different adverse conditions independently, but the ETR strategy presented in this paper can of course be applied to rainy and foggy conditions simultaneously, with rain having a strong impact on the braking distance, whereas fog impacts the probability of accident beyond the visibility distance.

In the following, we present the tests that we conducted on our test site to assess the feasibility of our method.

V. System Implementation and Demonstration

Earlier, the ETR strategy has been applied offline with data from an actual highway. Here, a real-time implementation of this ETR strategy is proposed in the framework of the French Dialogue Infrastructure Véhicules pour Améliorer la Sécurité routière (DIVAS) project initiated in 2007 [43]. First, the system and the experimental test site are described. Second, the equipment of the prototype vehicles is presented. Third, the outputs of the system in four different scenarios are given. Finally, the acceptability of the system is tackled.

A. DIVAS System

The global scheme of this vehicle–infrastructure integration (VII) project is shown in Fig. 14. This paper presents the in-vehicle comparison that is done to adapt speed to road characteristics (curvature, slope, and superelevation), vehicle characteristics (parameters such as the presence of an ABS or, possibly, tire quality), and environmental parameters that can only be estimated in real time (such as a wet road or limited visibility conditions triggered by rain, fog, or snow). Road characteristics fall within the competence of road operators as they are relatively permanent. They are transmitted to the car by servers next to the road. Here, the implementation of the system is presented, as well as the tests carried out on the test site of the French Institute of Science and Technology for Transport,

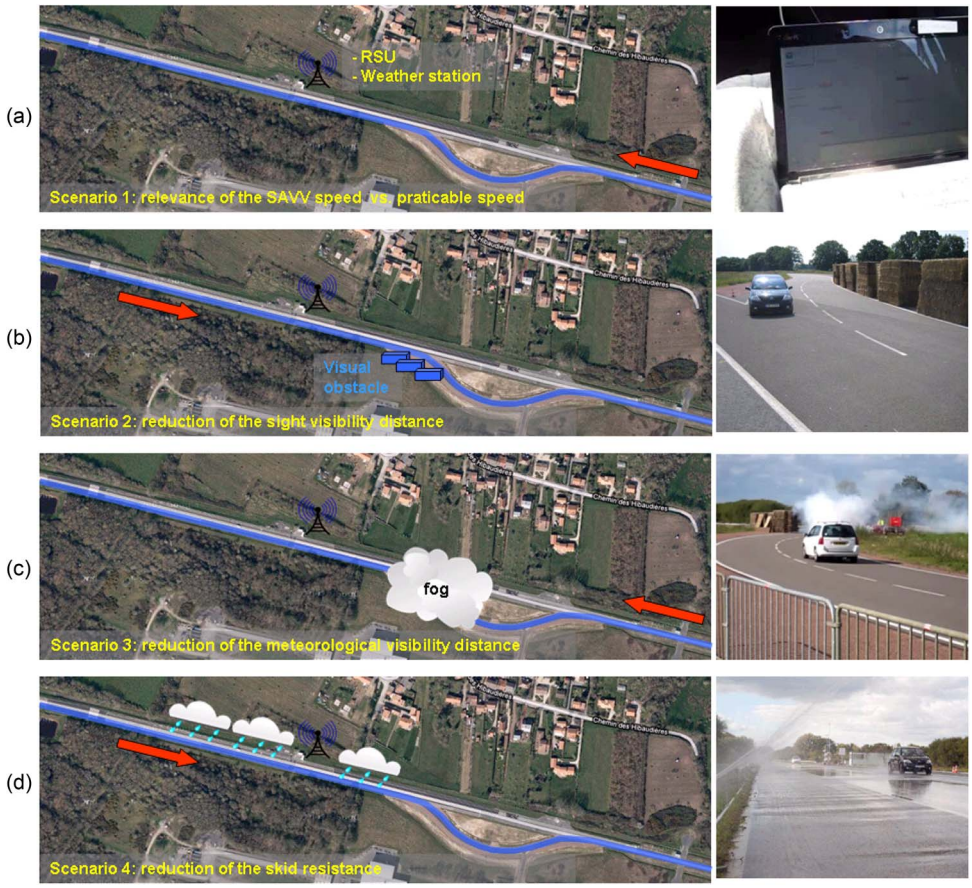

Fig. 15. Different test scenarios. (a) Relevance of the SAVV speed versus the practicable speed. (b) Reduction of the sight distance. (c) Reduction of the meteorological visibility distance. (d) Reduction of the skid resistance.

Spatial Planning, Development and Networks (IFSTTAR) in Nantes, France, to prove the technical feasibility of the system.

B. Test Site Description

To test and prove the feasibility of the DIVAS system, different tests were carried out. The most complex test took place on the test track of IFSTTAR in Nantes. This test track presents curves with different radii and road surfaces with different friction coefficients depending on the section. The test track was equipped with water sprinklers to simulate rain on one section, with a fog machine to simulate fog, and with maskings on the road side in some curves to simulate a local reduction of the geometric visibility, as shown in Fig. 15. The track was also equipped with five wireless access points, which are autonomous from the energy point of view due to solar cells. The weather station, which equipped the test site, was connected to the ad hoc network. An RSU was installed to monitor the test track. The characteristics of the test track were acquired by the CETE de Lyon using a dedicated mapping vehicle. The static data were map-matched and introduced into the RSU and the onboard unit (OBU). As there was no traffic on the test site, no V_{85} profile was available, and the reference speed profile issued from the Système d'Alerte de Vitesse excessive en approche de Virage (SAVV) model [44] was used instead. Fig. 16(a) shows the relevance and potential utility of a model of practiced speed, such as SAVV, when a reference profile cannot be estimated using the methodology exposed in Section IV-A.

C. Equipment of the Vehicles

To demonstrate the interest of V2I communications, two types of an OBU were implemented. The first type is merely a Netbook PC with a simple GPS unit. This simple OBU does not have access to the sensors of the vehicles and is representative of a personal navigation device. The second type is an expert OBU. It is integrated with the different sensors of the vehicle: camera, odometers, etc. This type of an OBU is able to collect exteroceptive data, such as rain or fog presence. It is representative of an integrated navigation system. Both types of OBUs were developed by teams from two different research institutes based on open standards. They were able to exchange data correctly with the same RSU. Five different vehicles were equipped, including a coach for public transport. The four cars could thus continuously and simultaneously transport observers to demonstrate the concept, whereas the coach could demonstrate for groups of people.

D. Test Scenarios

To show the effectiveness of the DIVAS system, four experimental scenarios were designed, which made use of the different subsystems and involved the five prototype vehicles simultaneously.

- The first scenario consisted in providing the driver with a speed recommendation in the case of good weather and

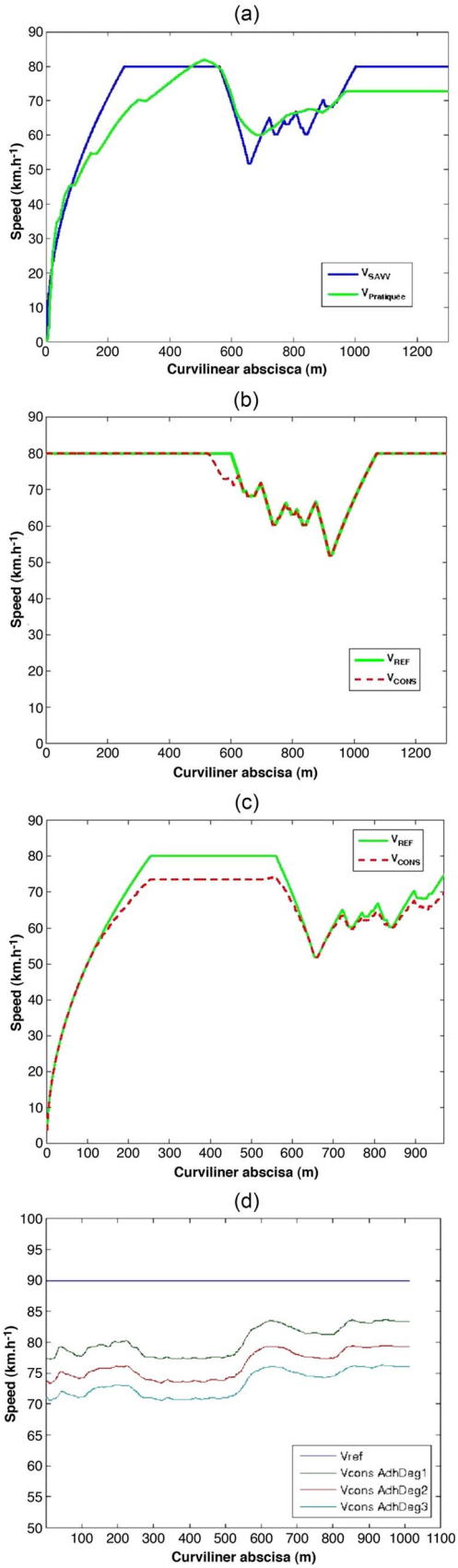

Fig. 16. Speed recommendation issued by the DIVAS system on the different test scenarios. (a) Speed profile in curve. (b) Speed profile in the case of reduced sight distance. (c) Speed profile in the case of reduced meteorological visibility. (d) Speed profile in the case of a wet road (with different levels of skid resistance).

a dry road. This scenario made use of the RSU, which communicates the reference speed to the vehicle. Recall that this speed depends on the road geometry, which was previously collected by a mapping vehicle.

- The second scenario consisted in reducing the sight distance of the driver using masking objects at the entrance of a curve. The sight distance can be computed based on 3-D data collected by dedicated mapping vehicles, following for instance the methodology proposed in [45].
- The third scenario consisted in reducing the meteorological visibility distance using a fog machine. The presence of fog was detected, and the meteorological visibility distance was estimated by the expert OBU using the camera along with the image processing technique proposed in [22]. This information was then transmitted to the RSU, which transmitted the information to simple OBUs.
- The fourth scenario consisted in reducing the skid resistance of the pavement by simulating rain with roadside sprinklers. The presence of rain was detected by an expert OBU. The information was transmitted to the RSU, which estimated the water layer thickness to estimate the skid resistance. The result was transmitted to all OBUs, which computed the final speed recommendation.

As one can see, these four scenarios make use of the different subsystems of DIVAS. They are shown in Fig. 15. On the left side of the figure, the scenario is recalled, and on the right side of the figure, a picture of the running demonstration is shown. Finally, in Fig. 16, the speed recommendations issued by the DIVAS system in the different scenarios are presented. Fig. 16(b) shows the local speed modulation proposed in a curve with sight distance reduced down to 50 m. The starting speed on the figure is not null since, in this scenario, cars are already at the speed limit before entering the straight section. Fig. 16(c) shows the speed modulation along the section when fog reduces the visual range. The density of the fog simulated was not constant on the whole track, but the proposed speed is computed using a constant meteorological visibility distance $V_{\mathrm{Met}} = 50$ m. Fig. 16(d) shows that, on a straight line, where a driver usually keeps its speed constant, the system is able to propose a speed that is modulated all along the driveway by accounting for the impact of the water on the different road surfaces. The rain simulated on the track using sprinklers was quite light, but the proposed speed is computed using the measured friction of the track under 3 mm of water height with the measuring vehicle described in Section IV-B.

In these scenarios, the accurate validation of the issued data was not of primary importance nor were the human–machine interaction issues. The goal was to demonstrate that all information introduced in the DIVAS system impacted the speed recommendation and thus in turn impacted the driving safety.

E. Acceptability

A complementary study has been carried out to analyze how the recommendations of the proposed device could be used and accepted by drivers [46]. “Acceptability” was understood

as "the conditions in which the system is good enough to satisfy the needs and requirements of actual and potential users" [47]. Relying on the Unified Theory of Acceptation and Use of Technology model [48], it has been shown that the will to use the device is correlated with the expected performances, the expected exertion, norms, and driving styles.

VI. Conclusion and Future Works

This paper has presented a new approach to computing an advisory speed to be used in an ISA system or an ADAS, by supervising the speed limit. By using measured characteristics of the road, accurate speed profiles during emergency braking are computed. The system proposed is able to deal with multiple adverse conditions that impair friction and visibility such as rain, fog, or both simultaneously. Vehicle and driver-related parameters, such as the presence of an ABS, the pressure on the brake pedal, or the perception–reaction time, can be used in our model of the vehicle dynamics. The presented method is open and can be extended to specific situations such as nighttime driving. It is also adaptable to the country, the network, and the population of drivers and vehicles, by using the relevant statistics. Finally, it can be improved by adding or modifiying models of the car dynamics, of the driver behavior, or the interaction between the environment, the infrastructure, the car, and the driver.

The novelty of this approach also comes from the use of a reference speed considered safe in ideal driving conditions. This speed is modulated in adverse conditions using potential accident severity criteria. Our advisory speed lies between the reference speed and the speed computed using previous works with a very cautious strategy based on the stopping distance.

In the end, three different advisory speeds are computed, which could be qualified as very cautious, cautious, and normal. When a speed is used in an ISA, it should be kept in mind that big differences from the legal speed or the current speed may have less impact and that the driver could be tempted to ignore the advise. Overcautious strategies can lead to less efficiency of an ISA, as shown in [49]. A much lower speed than the legal speed may also result in large speed differentials among the various drivers on the road and could lead to increased risk. As our method relies on a realistic and practiced speed and not on a model-driven approach, the proposed modulation of speed is less susceptible to leading to high differences of speed on the road. This point is essential and should be considered along with the adaptability of the proposed method to many factors related to the environmental conditions, the infrastructure, the vehicle, and the driver.

In the future, the method will be further extended using statistics for other types of crashes, such as "hit rigid fixed obstacles," "hit stopped cars," and "hit facing driving cars," with curves of the PI corresponding to these scenarios. We have to choose a strategy for setting parameters, such as perception–reaction time or pressure on the brake pedal. At the present time, these parameters are fixed, considering that $t_{\mathrm{PR}} = 1.2$ s corresponds to a good driver or, more carefully, $t_{\mathrm{PR}} = 2$ s as it is the 95th percentile of the perception–reaction time of drivers. This value of t_{PR} used in this example is driven from the reference value chosen for road design in France. It should be noted that this parameter is dependent on many factors, such as driver-related parameters, environmental conditions, and speed, for instance, and that our method allows for modification of this value, provided one has knowledge of the value of this parameter in specific conditions. Using accurate information on a specific driver could lead to advised speeds that suit the driver even better [50]. In this aim, relevant warnings are likely to improve user acceptance [51]. If the user acceptance is high enough, the safe speed profiles could be ultimately used in automotive cruise control systems in adverse weather conditions [52].

Acknowledgment

The authors would like to thank E. Dumont for helping with the revision of the manuscript, P. Lepert for his excellent management of the DIVAS project, CETE Normandie Centre for providing us with speed profiles along the road, and CETE Lyon for providing us with measured characteristics of the roads.

References

[1] "The global burden of disease: 2004 Update," World Health Organization (WHO), Geneva, Switzerland, Tech. Rep., 2008.
[2] A. Amditis, M. Da Lio, and R. Goudy, "Guest editorial special section on ITS and road safety," *IEEE Trans. Intell. Transp. Syst.*, vol. 11, no. 3, p. 524, Sep. 2010.
[3] "Traffic safety facts 2008," NHTSA, Washington, DC, USA, Tech. Rep., 2008.
[4] S. McLaughlin, J. Hankey, S. Klauer, and T. Dingus, "Contributing factors to run-off-road crashes and near-crashes," NHTSA, Washington, DC, USA, Tech. Rep. NPO-113, 2009.
[5] "The major data on accidentology," Nat. Road Safety Observatory, ONISR, Cedex, France, Tech. Rep., 2007.
[6] T. R. Centre, "Speed management," OECD/Eur. Conf. Ministers Transp., Paris, France, Tech. Rep., 2006.
[7] G. Nilsson, "The effect of speed limits on traffic accidents in Sweden," in *Proc. Int. Symp. Effects Speed Limits Traffic Accid. Transp. Energy Use, Org. Econom. Cooperation Dev.*, 1981, pp. 1–8.
[8] R. Elvik, "Speed and road accidents: An evaluation of the power model," Inst. Transp. Econom., Oslo, Norway, Tech. Rep., 2004.
[9] D. Finch, P. Kompfner, C. Lockwood, and G. Maycock, "Speed, speed limits and crashes," TRL, Crowthorne, U.K., Tech. Rep. 58, 1994.
[10] C. Kloeden, G. Ponte, and A. McLean, "Travelling speed and the risk of crash involvement on rural roads," Australian Transp. Safety Bureau, Canberra, ACT, USA, Tech. Rep. CR-204, 2001.
[11] O. Carsten and F. Tate, "External vehicle speed control—Final report: Integration," ITS, Univ. Leeds, Leeds, U.K., 2000.
[12] J. Ehrlich, F. Saad, S. Lassarre, and S. Romon, "Assessment of LAVIA speed adaptation systems: Experimental design and initial results on system use and speed behaviour," in *Proc. 13th ITS World Congr.*, London, U.K., 2006.
[13] A. Varhelyi and T. Makinen, "The effects of in-car speed limiters: Field studies," *Transp. Res. Part C, Emerg. Technol.*, vol. 9, no. 3, pp. 191–211, Jun. 2001.
[14] O. Carsten, F. Lai, K. Chorlton, P. Goodman, D. Carslaw, and S. Hess, "Speed limit adherence and its effect on road safety and climate change," Univ. Leeds—Inst. Transp. Studies, Leeds, U.K., Tech. Rep., Oct. 2008.
[15] R. Driscoll, Y. Page, S. Lassarre, and J. Ehrlich, "LAVIA—An evaluation of the potential safety benefits of the french intelligent speed adaptation project," in *Annu. Proc. Assoc. Adv. Automot. Med.*, 2007, vol. 51, pp. 485–505.
[16] N. Barnes, A. Zelinsky, and L. Fletcher, "Real-time speed sign detection using the radial symmetry detector," *IEEE Trans. Intell. Transp. Syst.*, vol. 9, no. 2, pp. 322–332, Jun. 2008.

[17] M. Ditze, F. Golatowski, N. Laum, A. Varhelyi, S. Gustafsson, and K. Geramani, "A survey on intelligen vehicle safety systems for adverse weather conditions," in *Proc. FISITA World Congr.*, 2010, pp. 1491–1498.
[18] C. Sentouh, S. Glaser, and S. Mammar, "Advanced vehicle-infrastructure-driver speed profile for road departure accident prevention," *Veh. Syst. Dyn.*, vol. 44, no. 1, pp. 612–623, 2006.
[19] E. Bertolazzi, F. Biral, M. Da Lio, A. Saroldi, and F. Tango, "Supporting drivers in keeping safe speed and safe distance: The saspence subproject within the european framework programme 6 integrating project PReVENT," *IEEE Trans. Intell. Transp. Syst.*, vol. 11, no. 3, pp. 525–538, Sep. 2010.
[20] A. Varhelyi, "Dynamic speed adaptation in adverse conditions—A system proposal," *IATSS Res.*, vol. 26, no. 2, pp. 52–59, 2002.
[21] F. Jimenez, F. Aparicio, and J. Paez, "Evaluation of in-vehicle dynamic speed assistance in Spain: Algorithm and driver behaviour," *IET Intell. Transp. Syst.*, vol. 2, no. 2, pp. 132–142, Jun. 2008.
[22] N. Hautière, J. P. Tarel, J. Lavenant, and D. Aubert, "Automatic fog detection and estimation of visibility distance through use of an onboard camera," *Mach. Vis. Appl. J.*, vol. 17, no. 1, pp. 8–20, Apr. 2006.
[23] R. Gallen, A. Cord, N. Hautière, and D. Aubert, "Towards night fog detection through use of in-vehicle multipurpose cameras," in *Proc. IEEE IV Symp.*, Baden-Baden, Germany, 2011, pp. 399–404.
[24] A. Cord and D. Aubert, "Towards rain detection through use of in-vehicle multipurpose cameras," in *Proc. IEEE IV Symp.*, Baden-Baden, Germany, 2011, pp. 833–838.
[25] J. Halimeh and M. Roser, "Raindrop detection on car windshields using geometric-photometric environment construction and intensity-based correlation," in *Proc. IEEE IV Symp.*, 2009, pp. 610–615.
[26] T. Teshima, H. Saito, M. Shimizu, and A. Taguchi, "Classification of wet/dry area based on the mahalanobis distance of feature from time space image analysis," in *Proc. IAPR Mach. Vis. Appl.*, 2009, pp. 467–470.
[27] E. Romano, T. Kelley-Baker, and R. Voas, "Female involvement in fatal crashes: Increasingly riskier or increasingly exposed?" *Accid. Anal. Prev.*, vol. 40, no. 5, pp. 1781–1788, Sep. 2008.
[28] L. Evans and P. Gerrish, "Antilock brakes and risk of front and rear impact in two-vehicle crashes," *Accid. Anal. Prev.*, vol. 28, no. 3, pp. 315–323, May 1996.
[29] D. Gabauer and H. Gabler, "Comparison of roadside crash injury metrics using event data recorders," *Accid. Anal. Prev.*, vol. 40, no. 2, pp. 548–558, Mar. 2008.
[30] D. Buzeman, D. Viano, and P. Lovsund, "Injury probability and risk in frontal crashes: Effects of sorting techniques on priorities for offset testing," *Accid. Anal. Prev.*, vol. 30, no. 5, pp. 583–595, Sep. 1998.
[31] E. Miltner and H. Salwender, "Influencing factors on the injury severity of restrained front seat occupants in car-to-car head-on collisions," *Accid. Anal. Prev.*, vol. 27, no. 2, pp. 143–150, Apr. 1995.
[32] S. Acierno, R. Kaufmanc, F. Rivara, and D. Grossman, "Vehicle mismatch: Injury patterns and severity," *Accid. Anal. Prev.*, vol. 36, no. 5, pp. 761–772, Sep. 2004.
[33] P. Mills and C. Hobbs, "The probability of injury to car occupants in frontal and side impacts," in *Proc. Stapp Car Crash Conf.*, Chicago, IL, USA, 1984, pp. 223–232.
[34] D. Gabauer and H. Gabler, "Comparison of the delta-v and occupant impact velocity crash severity metrics using event data recorders," in *Proc. 50th Annu. Assoc. Adv. Automotive Med. Conf.*, Chicago, IL, USA, 2006, pp. 57–71.
[35] R. Ross, J. Lenard, B. Hurley, P. Thomas, D. Otte, and G. Vallet, "Crash severity calculations—Theory and practice," in *Proc. STAIRS*, 1998, pp. 1–17.
[36] D. Wood, N. Veyrat, C. Simms, and C. Glynn, "Limits for survivability in frontal collisions: Theory and real-life data combined," *Accid. Anal. Prev.*, vol. 39, no. 4, pp. 679–687, Jul. 2007.
[37] D. Richards and C. Cuerden, "The relationship between speed and car driver injury severity," Transp. Res. Lab., London, U.K., Tech. Rep., 2009.
[38] L. Patte, "Evaluation du risque en relation avec la visibilité," in *Proc. Prévention Des Risques et Aides la Conduite*, 2010, pp. 65–74.
[39] A. Aly, E. S. Zeidan, A. Hamed, and F. Salem, "An antilock-braking systems (ABS) control: A technical review," *Intell. Control Autom.*, vol. 2, pp. 186–195, 2011.
[40] G. Louah, "The accuracy of a speed profile estimation method combining continuous and spot speed measurements," in *Proc. 13th Int. Conf. Road Safety Four Continents*, Warsaw, Poland, 2005, p. 8.
[41] S. Gormer, A. Kummert, S. B. Park, and P. Egbert, "Vision-based rain sensing with an in-vehicle camera," in *Proc. IEEE IV Symp.*, 2009, pp. 279–284.
[42] M. Kane and M. T. Do, "A contribution of elastohydrodynamic lubrification for estimation of tire-road friction in wet conditions," presented at the Int. Conf. Tribology, Parma, Italy, Sep., 2006, Paper AITC-AIT.
[43] N. Hautière and P. Lepert, "Dialogue between infrastructure and vehicles to improve road safety: The DIVAS approach," presented at the Transport Research Arena (TRA), Ljubljana, Slovenia, 2008.
[44] S. Glaser and V. Aguilera, "Vehicle-infrastructure-driver speed profile: Towards the next generation of curve warning systems," in *Proc. 10th World Congr. Exhib. Intell. Transp. Syst. Services*, Madrid, Spain, 2003.
[45] P. Charbonnier and J. P. Tarel, "On the diagnostic of road pathway visibility," presented at the Transport Research Arena (TRA), Brussels, Belgium, 2010.
[46] S. Bordel, C. Charon, N. Hautière, and A. Somat, "Acceptabilité d'un système embarqué," presented at the 54e Congrès de la Société Francaise de Psychologie, Montpellier, France, 2012.
[47] J. Nielsen, *Usability Engineering*. Boston, MA, USA: Academic, 1993.
[48] V. Venkatesh, M. Morris, G. Davis, and F. D. Davis, "User acceptance of information technology: Toward a unified view," *MIS Quart. Management Inf. Syst.*, vol. 27, no. 3, pp. 425–478, Sep. 2003.
[49] J. Blum and A. Eskandarian, "Managing effectiveness and acceptability in intelligent speed adaptation systems," in *Proc. IEEE ITSC*, Toronto, ON, Canada, 2006, pp. 319–324.
[50] E. Rendon-Velez, I. Horvath, and E. Opiyo, "Progress with situation assessment and risk prediction in advanced driver assistance systems: A survey," in *Proc. ITS World Congr.*, Stockholm, Sweden, 2009.
[51] F. Jimenez, Y. Liang, and F. Aparicio, "Adapting ISA system warnings to enhance user acceptance," *Accid. Anal. Prev.*, vol. 48, pp. 37–48, Sep. 2012.
[52] J. Daniel, G. Pouly, A. Birouche, J. P. Lauffenburger, and M. Basset, "Navigation-based speed profile generation for an open road speed assistant," in *Proc. 12th IFAC Symp. Control Transp. Syst.*, Redondo Beach, CA, USA, 2009, pp. 320–327.

Romain Gallen received both the M.S. degree in computer vision for industrial applications and the Ph.D. degree from Pierre and Marie Curie University, Paris, France, in 2005 and 2010, respectively.

From 2005 to 2007, he was an Engineer with the Laboratory on Interaction between Vehicle Infrastructure and Driver (LIVIC), French Institute of Science and Technology for Transport, Spatial Planning, Development, and Networks (IFSTTAR), Versailles, France. From 2007 to 2010, he was a Ph.D. student on visibility risk assessment in adverse weather conditions using computer vision at both LIVIC and the Laboratory for Road Operation, Perception, Simulations, and Simulators, IFSTTAR, Paris. Since 2011, he has been the Head of the Information Processing Unit with the Centre d'Etudes Techniques Maritimes et Fluviales, Plouzané, France, dealing with maritime transport safety.

Nicolas Hautière (M'13) received the M.S. degree in civil engineering from the National School of State Public Works, Lyon, France, in 2002; both the M.S. and Ph.D. degrees in computer vision from the University Jean Monnet, Saint Etienne, France, in 2002 and 2005, respectively; the Specialized Master degree in political science and sustainable development from École Nationale des Ponts et Chaussées, Paris, France, in 2013; and the Habilitation to Manage Research from the Université Paris-Est, Champs-sur-Marne, France, in 2011.

Since 2009, he has been a Research Leader with the Laboratory for Road Operation, Perception, Simulations and Simulators, French Institute of Science and Technology for Transport, Spatial Planning, Development and Networks, Paris, France. His research interests include the modeling of the meteorological phenomena reducing the highway visibility, the detection of visibility conditions, and the estimation of the visibility range.

Aurélien Cord received the Ph.D. degree in image processing for planetary surfaces with Toulouse University, Toulouse, France, in 2003.

In 2004, he was working on content-based image retrieval with Heudiasyc, Compiègne University, Compiègne, France. In 2005, he was working on the photometrical and spectral analysis of images from the Mars Express European mission with the European Space Agency, Paris, France. From 2006 to 2007, he was working on automatic characterization of textured images for defect detection on steel-plate images with Centre de Morphologie Mathématique, Mines ParisTech, Paris. Since 2008, he has been a Researcher with the Laboratory on Interaction between Vehicle Infrastructure and Driver, French Institute of Science and Technology for Transport, Spatial Planning, Development and Networks, Versailles, France, in computer vision applied to intelligent transportation systems. His research interests include analysis and interpretation of images and video from onboard cameras.

Sébastien Glaser received the Dipl.-Ing. degree from the National School of State Public Works, Vaulx en Velin, France, in 2000; the M.S. degree in image analysis and synthesis from Université Jean Monnet, Saint Etienne, France; and both the Ph.D. degree in automatic control, with emphasis on the vehicle dynamic analysis and the Habilitation to Manage Research from Université d'Evry, France, in 2004 and 2010, respectively.

He has been a Researcher with the Laboratory on Interaction between Vehicle Infrastructure and Driver, French Institute of Science and Technology for Transport, Spatial Planning, Development and Networks, Versailles, France, since 2004. He works on driving-assistance design and on driver studies. Since 2009, he has led a research team on risk analysis, decision-making, and control. He is currently involved in several European Union initiatives (i.e., eFuture and HAVEit) and leads a French initiative on low-speed automation (i.e., ANR-ABV).